

## CARDIOVASCULAR

## Proteomic signatures for perioperative oxygen delivery in skin after major elective surgery: mechanistic sub-study of a randomised controlled trial

Wendy E. Heywood<sup>1</sup>, Emily Bliss<sup>1</sup>, Fatima Bahelil<sup>2</sup>, Trinda Cyrus<sup>2</sup>, Marilena Crescente<sup>3</sup>, Timothy Jones<sup>2</sup>, Sadaf Iqbal<sup>4</sup>, Laura G. Paredes<sup>4</sup>, Andrew J. Toner<sup>5</sup>, Ana G. del Arroyo<sup>2</sup>, Edel A. O'Toole<sup>6</sup>, Kevin Mills<sup>1</sup> and Gareth L. Ackland<sup>2,\*</sup>

<sup>1</sup>Translational Mass Spectrometry Research Group, UCL Institute of Child Health, London, UK, <sup>2</sup>Translational Medicine & Therapeutics, William Harvey Research Institute, Queen Mary University of London, London, UK, <sup>3</sup>Department of Life Sciences, Manchester Metropolitan University Manchester, UK, <sup>4</sup>University College London NHS Hospitals Trust, London, UK, <sup>5</sup>Department of Anaesthesia, Royal Perth Hospital, Perth, Western Australia, Australia and <sup>6</sup>Centre for Cell Biology and Cutaneous Research, Blizard Institute, Queen Mary University of London, London, UK

\*Corresponding author. E-mail: [g.ackland@qmul.ac.uk](mailto:g.ackland@qmul.ac.uk)



This article is accompanied by an editorial: Lifting the lid on perioperative goal-directed therapy by D.S Martin, *Br J Anaesth* 2021;127:508–510, doi: [10.1016/j.bja.2021.07.009](https://doi.org/10.1016/j.bja.2021.07.009)

### Abstract

**Background:** Maintaining adequate oxygen delivery (DO<sub>2</sub>) after major surgery is associated with minimising organ dysfunction. Skin is particularly vulnerable to reduced DO<sub>2</sub>. We tested the hypothesis that reduced perioperative DO<sub>2</sub> fuels inflammation in metabolically compromised skin after major surgery.

**Methods:** Participants undergoing elective oesophagectomy were randomised immediately after surgery to standard of care or haemodynamic therapy to achieve their individualised preoperative DO<sub>2</sub>. Abdominal punch skin biopsies were snap-frozen before and 48 h after surgery. On-line two-dimensional liquid chromatography and ultra-high-definition label-free mass spectrometry was used to characterise the skin proteome. The primary outcome was proteomic changes compared between normal ( $\geq$ preoperative value before induction of anaesthesia) and low DO<sub>2</sub> ( $<$ preoperative value before induction of anaesthesia) after surgery. Secondary outcomes were functional enrichment analysis of up/down-regulated proteins (Ingenuity pathway analysis; STRING Protein-Protein Interaction Networks). Immunohistochemistry and immunoblotting confirmed selected proteomic findings in skin biopsies obtained from patients after hepatic resection.

**Results:** Paired punch skin biopsies were obtained from 35 participants (mean age: 68 yr; 31% female), of whom 17 underwent oesophagectomy. There were 14/2096 proteins associated with normal ( $n=10$ ) vs low ( $n=7$ ) DO<sub>2</sub> after oesophagectomy. Failure to maintain preoperative DO<sub>2</sub> was associated with upregulation of proteins counteracting oxidative stress. Normal DO<sub>2</sub> after surgery was associated with pathways involving leucocyte recruitment and upregulation of an antimicrobial peptidoglycan recognition protein. Immunohistochemistry ( $n=6$  patients) and immunoblots after liver resection ( $n=12$  patients) supported the proteomic findings.

**Conclusions:** Proteomic profiles in serial skin biopsies identified organ-protective mechanisms associated with normal DO<sub>2</sub> after major surgery.

**Clinical trial registration:** ISRCTN76894700.

**Keywords:** oxygen delivery; proteomics; randomised controlled trial; sepsis; skin; surgery; wound infection

Received: 30 September 2020; Accepted: 1 June 2021

© 2021 British Journal of Anaesthesia. Published by Elsevier Ltd. All rights reserved.  
For Permissions, please email: [permissions@elsevier.com](mailto:permissions@elsevier.com)

**Editor's key points**

- Adequate oxygen delivery in the perioperative period is essential to minimising organ dysfunction and injury.
- This study used proteomic analysis to test the effects of reduced perioperative oxygen delivery on inflammation in skin biopsies obtained after major surgery in high-risk patients.
- Failure to maintain preoperative oxygen delivery after surgery was associated with upregulation of proteins counteracting oxidative stress, whereas normal oxygen delivery was associated with pathways involving leucocyte recruitment and inflammation.
- These findings in high-risk surgical patients reveal a link between low oxygen delivery, oxidative stress, and reparative processes that may provide mechanistic insight into organ injury and potential precision medicine-guided therapies after surgery.

Mass spectrometry (MS)-based proteomics provide novel information that is not discernible through genomic analyses alone.<sup>1</sup> Enzymatic digestion of proteins extracted from biological samples into peptides enables analysis by liquid chromatography–tandem MS (LC-MS/MS). Briefly, LC-MS/MS quantifies proteins by the mass-to-charge ratio of ionised peptides, or fragments of peptides. Computational algorithms identify proteins by correlating known masses with the spectra of the signal intensity of detected ions as a function of the mass-to-charge ratio.<sup>2</sup> Other than a single study of plasma proteomics,<sup>3</sup> no perioperative studies have thus far used proteomics to examine serial changes at the end-organ level.

Complications after elective oesophagectomy and major intra-abdominal surgery occur in ~20% of patients, resulting in delayed discharge, readmission to hospital, or both.<sup>4</sup> Avoiding even minor complications after major surgery appears to be pivotal in determining survival, extending until after hospital discharge.<sup>5</sup> Maintaining oxygen delivery (DO<sub>2</sub>) is strongly associated with minimising organ dysfunction and reducing morbidity after surgery.<sup>6–9</sup> Although the mechanisms that trigger complications associated with the failure to preserve DO<sub>2</sub> remain unclear, the intersection between metabolic dysfunction and inflammation may be key.<sup>10,11</sup>

Skin is particularly vulnerable to reductions in cardiac output and hence DO<sub>2</sub>, as blood is preferentially shunted away from skin to preserve the perfusion of vital organs.<sup>12</sup> Direct injury to the skin triggers an immunometabolic response that coordinates wound healing.<sup>13</sup> Even after distant injury, cytokine production is upregulated in uninjured skin from a range of skin-resident cells.<sup>14</sup> Skin-derived mediators contribute to systemic inflammation and organ dysfunction through lymph node drainage.<sup>15</sup> The skin proteome may, therefore, reveal mechanistic insight into how organs are impacted by reduced DO<sub>2</sub> after major surgery.

We tested the hypothesis that reduced DO<sub>2</sub> after major surgery fuels organ injury through inflammation generated by metabolically compromised skin. We used LC-MS/MS to serially quantify the skin proteome in patients enrolled in an RCT that demonstrated that morbidity was less frequent in patients in whom preoperative DO<sub>2</sub> values were maintained after surgery (regardless of goal-directed haemodynamic therapy).<sup>8</sup>

**Methods****Subjects**

Adult patients undergoing major elective surgery who were enrolled in the Postoperative Morbidity Oxygen delivery (POM-O) study gave written informed consent for skin biopsy samples to be obtained. POM-O was a multicentre, double-blind, RCT done in four university hospitals in the UK (ISRCTN76894700), approved by the South London Research Ethics Committee Office (09/H0805/58).<sup>6</sup>

**Inclusion criteria**

Patients undergoing surgery expected to last  $\geq 120$  min were eligible for recruitment provided they satisfied the following high-risk criteria: ASA physical status classification  $\geq 3$ ; surgical procedures with an estimated or documented risk of postoperative morbidity (as defined by the Postoperative Morbidity Survey)  $> 50\%$ ; modified Revised Cardiac Risk Score of  $\geq 3$ , as defined by age  $\geq 70$  yr, a history of cardiovascular disease (myocardial infarction, coronary artery disease, cerebrovascular accident, electrocardiographic evidence for established cardiac pathology), cardiac failure, poor exercise capacity (anaerobic threshold  $< 11$  ml kg<sup>-1</sup> min<sup>-1</sup> assessed by cardiopulmonary exercise testing or Duke Activity Status Index), renal impairment (serum creatinine  $\geq 130$   $\mu$ M), or diabetes mellitus.

**Exclusion criteria**

Refusal of consent, pregnancy, lithium therapy or allergy, recent myocardial ischaemia (within the previous 30 days), acute arrhythmia, acute bleeding, and patients receiving palliative treatment only.

**Intervention**

Patients were allocated by computer-generated randomisation to a postoperative protocol (i.v. fluid, with and without dobutamine) targeted to achieve their individual preoperative DO<sub>2</sub> value (goal-directed therapy) or standardised care (control). Patients and staff were masked to the intervention. The primary outcome of the original parent study was absolute risk reduction in morbidity (defined by Clavien-Dindo grade II or more)<sup>16</sup> on postoperative Day 2.

**Skin biopsy and sample preparation**

We obtained 2 mm skin punch biopsies (Instrapac, Robinson Healthcare, Worksop, UK) before surgery within 5 cm of the surgical incision immediately after the induction of general anaesthesia (Fig. 1). A repeat biopsy was obtained 48 h after surgery on the opposite side of the surgical incision (under local anaesthesia). Punch biopsies were immediately snap-frozen in liquid nitrogen or immersed in paraformaldehyde 4%. For proteomic analyses, samples were prepared as described.<sup>17</sup> Snap-frozen samples were homogenised in ammonium bicarbonate 50 mM and ASB-14 2% w/v using bead (Precellys 1.4 mm diameter ceramic beads, Peqlab, VWR, Lutterworth, UK) and mechanical homogenisation (Minilys®, Bertin Technologies, Montigny-le-Bretonneux, France). A modified Lowry protein assay (Pierce™, ThermoFisher Scientific, Loughborough, UK) was used to calculate the protein

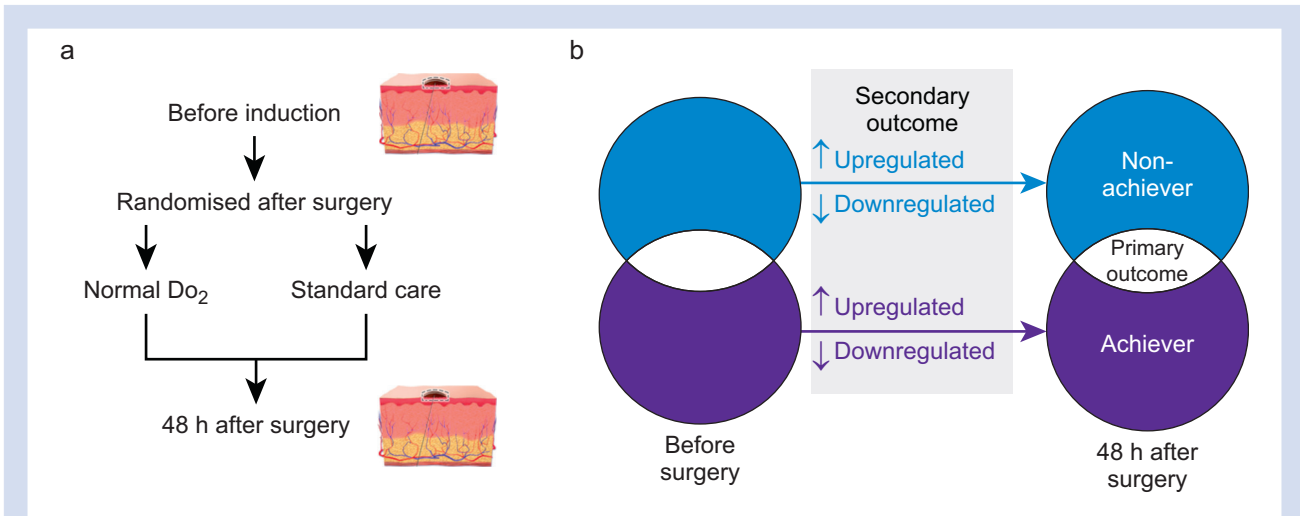


**Fig 1.** Methods and analysis. (a) Schematic showing timing of serial skin biopsies before induction of anaesthesia and 48 h after the haemodynamic trial intervention. (b) Venn diagram showing primary and secondary outcome analyses. Blue shading/text denotes patients in whom oxygen delivery (DO<sub>2</sub>) remained low after intervention. Red shading/text denotes subjects in whom DO<sub>2</sub> was normal after intervention. Primary outcome was comparison between proteins differentially expressed in patients with normal vs low DO<sub>2</sub> after intervention. Grey shaded area highlights secondary pathway analyses which accounted for directional changes in protein expression for subjects with normal or low DO<sub>2</sub> value. An increase/decrease was defined by fold-change >1.5, confidence score >20 and P-value <0.05 (analysis of variance, ANOVA), as generated by Progenesis QI analysis software (Nonlinear Dynamics, Newcastle upon Tyne, UK).

content, and 50 µg was lyophilised and resolubilised in TRIS-HCl 100 mM, pH 7.8, containing ASB-14 2% w/v, urea 6 M and thiourea 2 M, and digested using Sequencing Grade Modified Trypsin (Promega, Madison, WI, USA).

### Two-dimensional liquid chromatography

After in-solution digestion of the homogenised sample, purification of digested sample peptides by reverse phase C-18 chromatography was undertaken to remove the salt and lipid content (ISOLUTE® C18 columns, Biotage, Ystrad Mynach, UK), as described.<sup>17</sup> Then, two-dimensional high pH fractionation of sample peptides, followed by low pH chromatographic separation using an online nanoAcquity ultra high performance liquid chromatography system was undertaken (Supplementary data). For each fraction, a 60 min MS analysis was performed on a SYNAPT G2-Si mass spectrometer (Waters, Manchester, UK) in a UDMS<sup>E</sup> positive ion electrospray ionisation mode.<sup>18</sup>

### Proteomic analysis

Raw MS data were processed using Progenesis QI analysis software (Nonlinear Dynamics, Newcastle-Gateshead, UK). Peptide identification was performed using MS<sup>E</sup> search identification against the Uniprot Human reference proteome 2015, with one missed cleavage and 1% peptide false discovery rate (FDR).<sup>19</sup> Fixed modifications were set to carbamidomethylation of cysteines and dynamic modifications of hydroxylation of aspartic acid, lysine, asparagine, and proline and oxidation of methionine. A protein was considered to be differentially expressed if there was a significant change ( $P < 0.05$ ) from preoperative values accounting for the degree, direction, and rank of difference between samples obtained before and 48 h after surgery with sequence length  $\geq 6$ , hits  $\geq 2$ , maximal mean fold change  $\geq 1.5$ , and >20 confidence score, a further measure of FDR (Progenesis QI, Elstree, UK). Proteomics data were

deposited in the PRoteomics IDentifications (PRIDE) public-domain repository, which provides a single point for submitting MS-based proteomics data.<sup>20</sup> Data were normalised and significance determined by one-way analysis of variance (Progenesis QI).

### Immunohistochemistry

Immunofluorescence on frozen sections of human skin biopsies was used to confirm selected findings from the proteomic data by histologists masked to clinical details (Atlantic Bone Screen, Saint-Herblain, France). Using validated antibodies (Supplementary data), protein expression of epidermal integrin alpha-6 (ITGA6; 1:50; Merck Millipore [MAB1378], Watford, UK) and the cell surface glycoprotein CD44 (1:50; Novocastra [BMS144], Leica Microsystems, Milton Keynes, UK) were quantified by immunofluorescence by an investigator masked to clinical details (Fiji software, NIH Image, Bethesda, MD, USA).

### Immunoblots

Membranes were incubated with the following species-specific primary antibodies for parkin and superoxide dismutase-1 to confirm selected findings from the proteomic data, which were masked to clinical details. Secondary antibodies (1:2000) were rabbit anti-mouse HRP (Dako, Stockport, UK) or goat anti-rabbit HRP (Cell Signaling Technology, Leiden, The Netherlands), as indicated. Membranes were developed using ECL<sup>TM</sup> reagent and Hyperfilm ECL (Amersham, Little Chalfont, UK).

### Primary outcome

The primary outcome was differential protein expression (before vs after surgery), compared between individuals with

DO<sub>2</sub> defined as normal (same or higher than each individual's preoperative value) or low (less than each individual's preoperative value).

### Secondary outcomes: functional pathway analysis

We assessed categorical changes in skin protein expression (as defined by fold change and confidence scores) before and after surgery using the STRING database, which collects, scores and integrates all publicly available sources of protein–protein interaction information through which computational predictions for direct (physical) and indirect (functional) interactions are made.<sup>21</sup> For the enrichment analysis, STRING uses the established classification systems Gene Ontology<sup>22</sup> and KEGG<sup>23</sup> but also offers additional, new classification systems based on high-throughput text-mining and on a hierarchical clustering of the association network itself. To compare quantitative fold changes in protein expression between DO<sub>2</sub> achievers vs non-achievers, we used Ingenuity Pathways Analysis (IPA) (01–13) software (Qiagen, Manchester, UK) to perform enrichment analyses<sup>24</sup> to estimate the significance of observing a candidate protein set within the context of biological systems.<sup>25</sup> Protein identifiers were mapped in the Ingenuity Pathway Knowledge Base to find cellular functions and diseases significantly associated with differentially expressed proteins. We determined changes in biological processes associated with differential protein expression by

using downstream effect analysis. Molecular interactions between proteins and affected functions were assessed using network analysis.

### Statistical analysis

All analyses were conducted by investigators blinded to the identity of treatments/genotypes. Clinical data were processed by analysers blinded to patient group assignments. For statistical testing, the Benjamin-Hochberg procedure was applied where applicable to correct for testing multiple hypotheses. Data distribution was assessed by the Kolmogorov–Smirnov normality test. *P*-values <0.05 were considered significant.

### Sample size estimation

We estimated that 20 paired samples would achieve a power of 80% ( $\alpha=0.05$ ) to detect an effect size of 0.7 between pairs where protein expression changed by  $\geq 1.5$ -fold (confidence score >20).

## Results

### Participant characteristics

Paired punch skin biopsy samples were obtained before and 48 h after surgery from 35 participants (Fig. 2) who

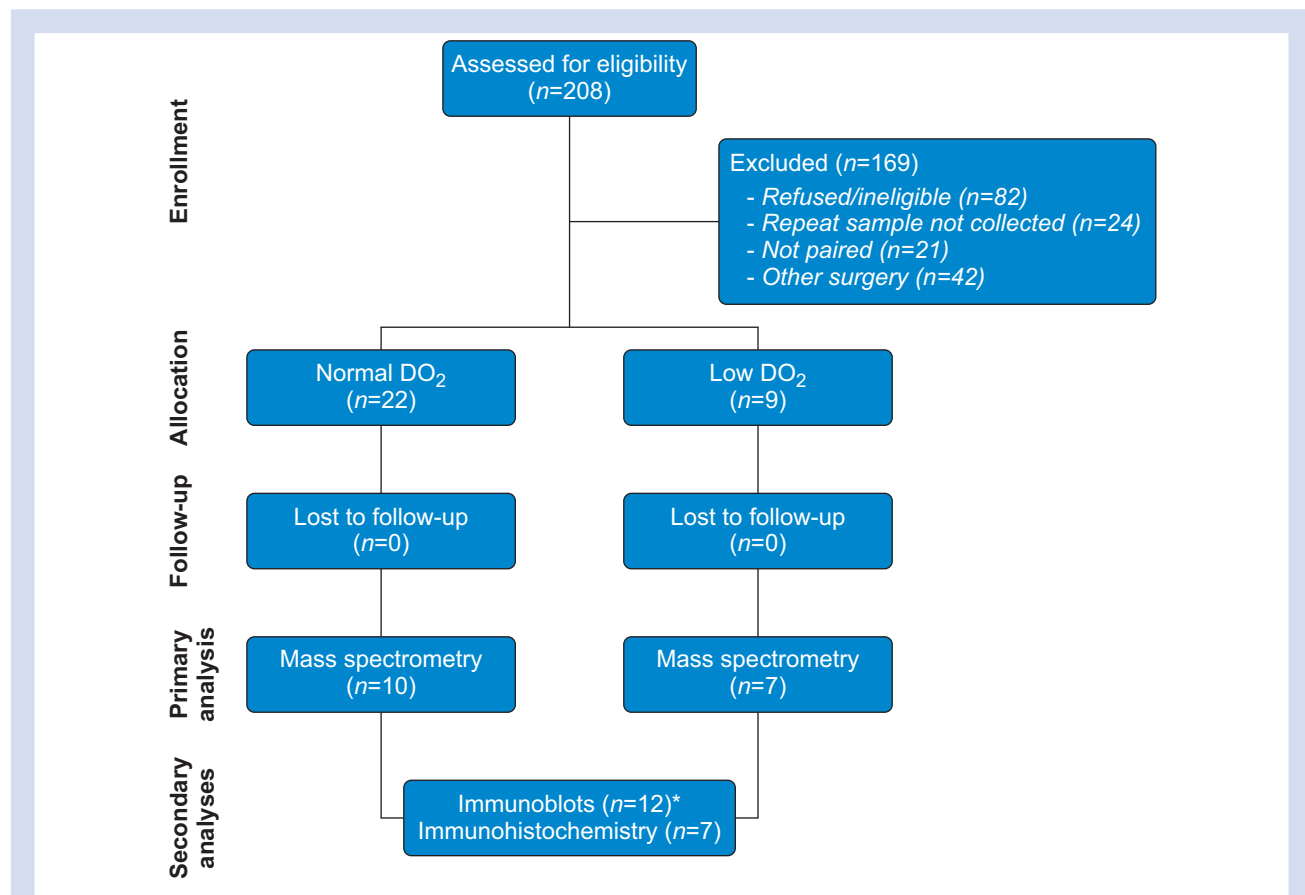
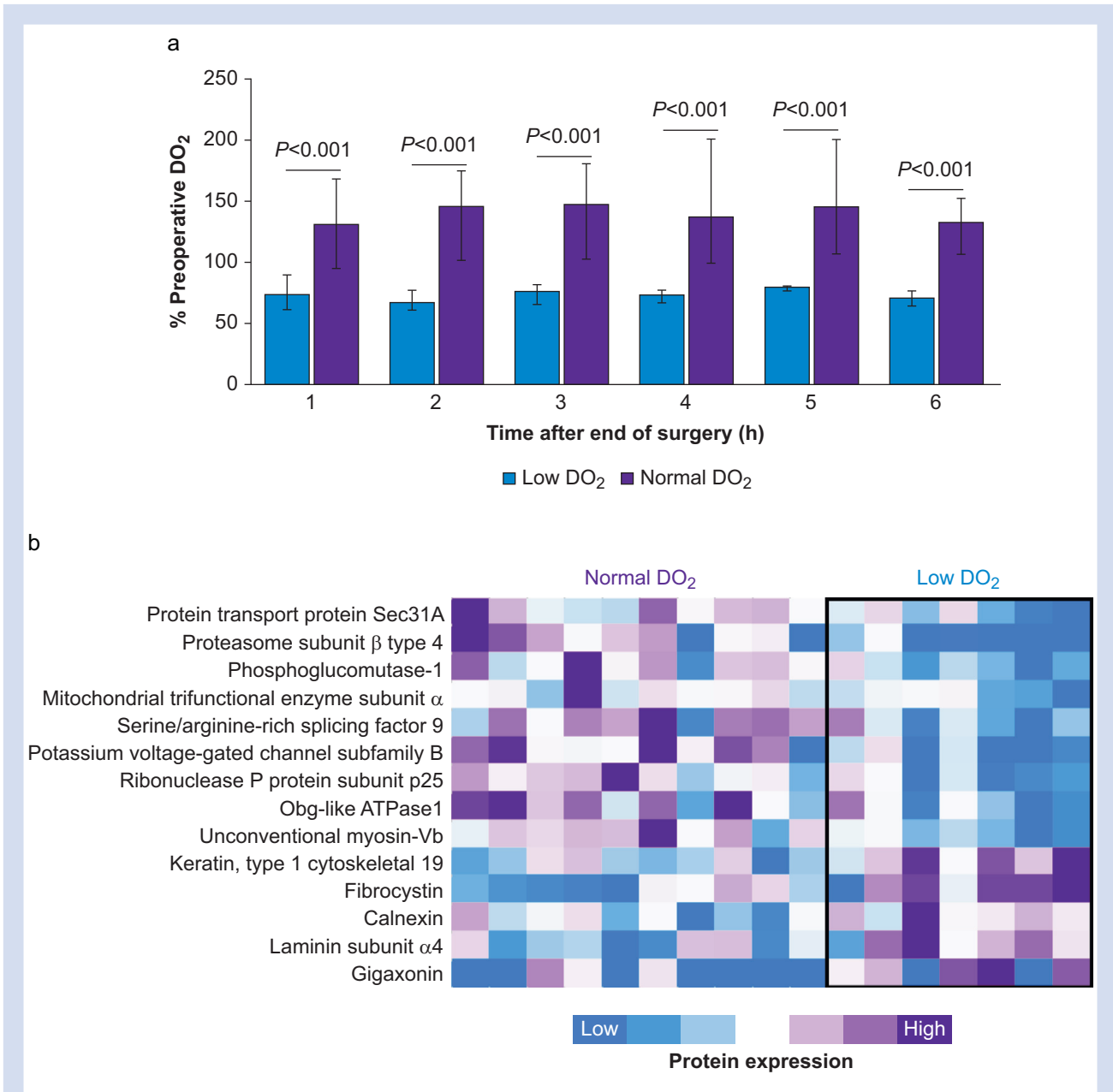


Fig 2. Recruitment of participants into skin biopsy sub-study. Asterisk denotes three paired samples that were used for proteomics and immunoblotting (biopsies were divided in half).



**Fig 3.** Proteomic differences in skin associated with perioperative oxygen delivery. (a) Oxygen delivery (DO<sub>2</sub>) expressed as percentage of preoperative DO<sub>2</sub> (measured before induction of anaesthesia). P-values refer to comparison between subjects with normal vs low DO<sub>2</sub> over each hour during the 6 h intervention period after surgery. (b) Identification of 14 proteins that were differentially expressed after surgery in non-DO<sub>2</sub> achievers and DO<sub>2</sub> achievers (median confidence score 63.7 [27.1–128.5]). Heatmap data are shown for relative changes for within-protein comparisons, for subjects with normal vs low DO<sub>2</sub> during trial intervention.

underwent oesophagectomy or liver resection (mean age 68 yr); 31% female; [Supplementary data](#)). No biopsy sites became infected. Subjects who failed to achieve normal DO<sub>2</sub> were more likely to sustain serious complications (including sepsis) after surgery ([Fig. 3a](#)), compared with 14/27 (51.8%) subjects who achieved their individualised preoperative DO<sub>2</sub> target (absolute risk reduction 36% [95% confidence interval 6–65%]).

#### Primary outcome: protein expression after surgery, stratified by DO<sub>2</sub>

Label-free proteomic analysis was undertaken in 17 subjects who underwent oesophagectomy ([Table 1](#)). We identified 2096 proteins in skin biopsy samples, of which 157 were differentially expressed  $\geq 1.5$ -fold after surgery independent of DO<sub>2</sub> (median confidence score 124 [62–252]; [supplementary data](#)).

**Table 1** Subject characteristics. Data shown for participants who underwent goal-directed therapy after oesophagectomy or hepato-biliary surgery aimed at achieving their preoperative oxygen delivery and had paired skin biopsies taken. Data are presented as mean (standard deviation) for parametric data and as median (25th–75th inter-quartile range) for non-parametric data. Frequencies are presented with percentages (%). Age is rounded to the nearest year. \*Indicates sepsis or suspected infection within 72 h of surgery. <sup>†</sup>Inhalation general anaesthesia was used in all cases.

	Skin biopsies (oesophagectomy)		All participants	
	Normal DO <sub>2</sub> (n=10)	Low DO <sub>2</sub> (n=7)	Normal DO <sub>2</sub> (n=22)	Low DO <sub>2</sub> (n=9)
Age (yr)	67 (6)	67 (4)	71 (10)	69 (4)
Female sex (n; %)	4 (31)	3 (43)	10 (45)	4 (44)
Body mass index (kg m <sup>-2</sup> )	28.5 (4.0)	28.4 (2.8)	27.7 (4.1)	28.3 (4.0)
Haemoglobin (g L <sup>-1</sup> )	121 (15)	139 (20)	125 (15)	135 (23)
Albumin (g L <sup>-1</sup> )	42 (5)	45 (2)	44 (5)	44 (3)
<b>Co-morbidities, n (%)</b>				
Cardiovascular disease	12 (71)	4 (57)	19 (86)	7 (78)
Diabetes mellitus	3 (18)	0	5 (23)	1 (11)
Hypertension	8 (47)	3 (43)	14 (64)	5 (56)
<b>Intraoperative</b>				
General <sup>†</sup> + epidural anaesthesia	11 (65)	7 (100)	17 (77)	8 (89)
Duration of operation (min)	260 (195–335)	298 (288–360)	273 (102)	319 (83)
Fluid therapy (ml kg <sup>-1</sup> h <sup>-1</sup> )	7.1 (4.8–11.7)	8.8 (7.3–10.6)	9.6 (6.3–14.5)	11.3 (4.1)
Packed red cells, n (%)	3 (18)	1 (14)	1	1
Lactate (mM)	2.4 (1.2–3.0)	1.8 (1.7–2.4)	1.7 (1.2–2.6)	2.1 (1.7–2.4)
<b>Intervention period</b>				
Dobutamine	3 (30)	1 (14)	5 (23)	1 (11)
Fluid therapy (ml kg <sup>-1</sup> h <sup>-1</sup> )	20.5 (16.5–25.0)	16.9 (12.9–23.0)	18.4 (13.1–24.7)	21.2 (15.4–24.8)
Packed red cells, n (%)	2 (22)	0	2 (9)	3 (33)
Lactate (mM)	2.4 (1.2–3.0)	1.8 (1.7–2.4)	1.9 (0.9–2.6)	1.3 (1.2–2.5)
Haemoglobin (g L <sup>-1</sup> )	114 (18)	122 (18)	113 (16)	114 (22)
<b>Complications</b>				
Clavien-Dindo >grade 2, n (%)	5 (50)	5 (74)	11 (50)	6 (67)
Infection/sepsis*, n (%)	5 (50)	4 (57)	7 (32)	5 (56)
Length of hospital stay (days)	16 (10–27)	24 (17–78)	12 (8–17)	17 (12–22)

Fourteen out of 2096 detected proteins distinguished normal (n=10) vs low (n=7) DO<sub>2</sub> values after oesophagectomy (as illustrated by the heatmap in Fig. 3b).

### Secondary outcomes: systems analysis

To further dissect potential molecular interactions using Ingenuity Pathway Analysis (Fig. 4a), we directly compared expression proteins before and after surgery for subjects who had either normal or low DO<sub>2</sub> after the trial intervention. In 10 subjects with normal DO<sub>2</sub>, the expression of 65 proteins differed after surgery. In subjects with low DO<sub>2</sub> values (n=7), 92 proteins changed after surgery (median confidence score 116 [62–223]); Supplementary data). Pathways involved in nervous system and renal injury were activated in patients with low DO<sub>2</sub> (Fig. 4b). In skin, we found that proteins involved in leucocyte activation and smooth muscle migration pathways (Fig. 4c) were upregulated in subjects with normal DO<sub>2</sub>. In particular, increased expression of the antimicrobial bactericidal peptidoglycan recognition protein-1 (PGLYRP-1) was observed.<sup>26,27</sup> By contrast, in subjects with low DO<sub>2</sub>, proteins involved in epithelial necrosis with established roles in oxidative stress (superoxide dismutase-1, DJ-1/PARK7) and wound healing (CD44, thrombospondin, plasminogen, retinal binding protein-4) were differentially expressed compared with achievers (Fig. 4c).

### Immunohistochemical and immunoblot confirmation of proteomic findings

To establish the generalisability of the proteomic data from skin biopsies obtained after oesophagectomy, separate

external validation of specific proteins was undertaken. We randomly selected skin biopsies from six subjects obtained before and after hepatic surgery for protein quantification by immunohistochemistry. We focused on proteins identified by MS for which there were antibodies that have been validated for skin immunohistochemistry (Fig. 5a). Expression levels of CD44 (the principal cell surface receptor for hyaluronate) and  $\alpha 6 \beta 4$  integrin (which stabilises skin through the formation of hemidesmosomes) were reduced after surgery (Fig. 5b). These changes were mirrored by semi-quantitative immunoblots and were also found in a murine model of hepatectomy (Supplementary data).

### Discussion

Serial proteomic analysis of skin biopsies in high-risk surgical patients revealed a link between low DO<sub>2</sub>, oxidative stress, and reparative processes previously identified by gene knockout experiments. The proteomic data were verified by immunohistochemistry using selected antibodies that have been validated for immunohistochemistry in skin. Taken together, these data show that serial skin biopsies provide mechanistic insight into organ injury after surgery.

The complex composition in skin of proteins, metabolites, and lipids, coupled with immunological surveillance and neural innervation, has led to frequent use of skin biopsies to aid diagnosis of several hereditary neurologic metabolic diseases.<sup>28</sup> Thus, insights into numerous genetic diseases have been afforded by skin biopsies, even though the disease does not primarily affect skin. However, despite the accessibility of skin, human proteomic studies are scarce.<sup>29</sup> In part, this

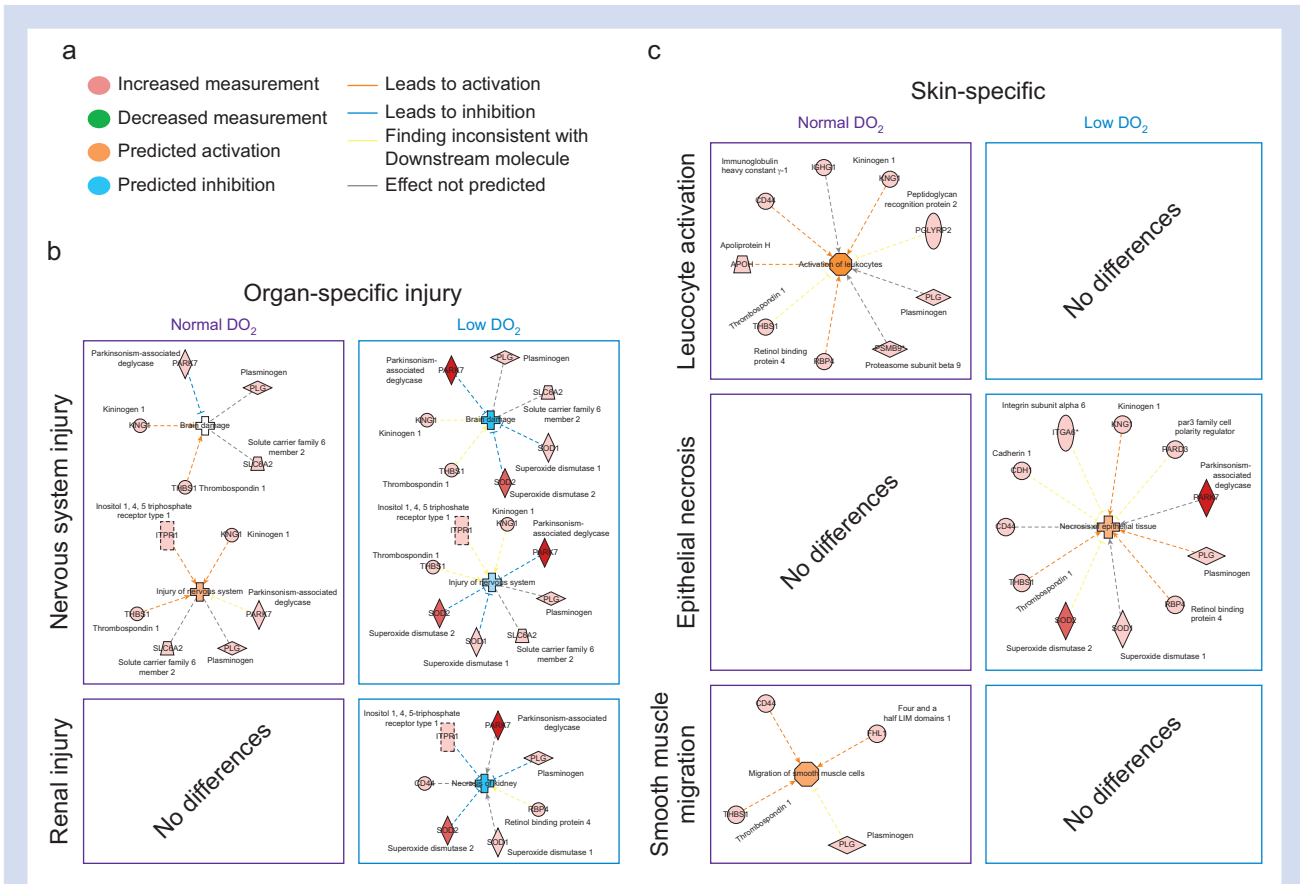


**Fig 4.** Postoperative differences in protein expression related to oxygen delivery intervention. (a) Key for bioinformatic prediction of up/downregulated proteins, activation or inhibition of protein function, or both. (b) Canonical pathway analysis for enriched signalling target categories in organ-specific injury pathways identified through differential proteins expression in subjects in whom oxygen delivery (DO<sub>2</sub>) target was achieved vs non-achievers. (c) Canonical pathway analysis for enriched signalling categories in skin-specific pathways for subjects who achieved or failed to achieve their individualised preoperative DO<sub>2</sub> value.

reflects that skin has presented significant challenges for conventional proteomic techniques because of its high lipid content, insolubility, and extensive cross-linking of proteins, all of which complicate the isolation and digestion of proteins for analysis using MS techniques.<sup>17</sup> This study was facilitated by recent advances in on-line fractionation and optimised acquisition protocols utilising ion mobility separation technology, which has increased the scope for protein identification more than 10-fold from a single punch biopsy.<sup>17</sup> Our study extends previous proteomic analysis of plasma obtained from older adults undergoing elective surgery, which identified 564 proteins with altered expression levels altered after surgery.<sup>3</sup> Tracking proteomic changes using skin biopsies is acceptable to surgical patients, easy to perform, and provides integrated mechanistic insights into end-organ physiology that is seldom reflected by changes in circulating proteins in blood.

The proteomic profiles revealed by our study have captured components from each of the four dynamic overlapping processes required for the coordination of successful healing of skin wounds.<sup>30</sup> Briefly, haemostasis is triggered once platelets encounter collagen and the extracellular matrix. The development of fibrin clots and release of clotting factors, growth factors, and cytokines initiate the inflammatory phase, which

lasts for ~48 h (i.e. the timeframe over which the two skin punch biopsies were obtained). The inflammatory phase is heralded by the chemotaxis of neutrophils and monocyte/macrophages to commence phagocytosis of cellular debris and pathogens, assisted by activation of mast cells and fibroblasts. New extracellular matrix is then created by deposition of collagen by fibroblasts and further remodelling facilitated by transforming growth factor-β, proteoglycans, fibronectin, and protease inhibitors.<sup>31</sup> Our proteomic profiling ceased before the process of proliferation and epithelialisation is widely held to be completed, which requires angiogenesis and neovascularisation.

Canonical pathway analysis highlighted that acute phase proteins and sirtuin signalling were markedly upregulated in subjects with low DO<sub>2</sub>, suggesting that reduced DO<sub>2</sub> results in significant metabolic compromise. The sirtuins are a family of NAD<sup>+</sup>-dependent class III histone deacetylases regulating the metabolic and transcriptomic response to oxidative stress in skin.<sup>20</sup> Activation of sirtuins 1–3 accelerates wound healing.<sup>32</sup> At the individual protein level, we found coordinated upregulation of antioxidant proteins including mitochondrial heat shock protein deglycase DJ-1 and the mitochondrial antioxidant manganese superoxide dismutase. These changes

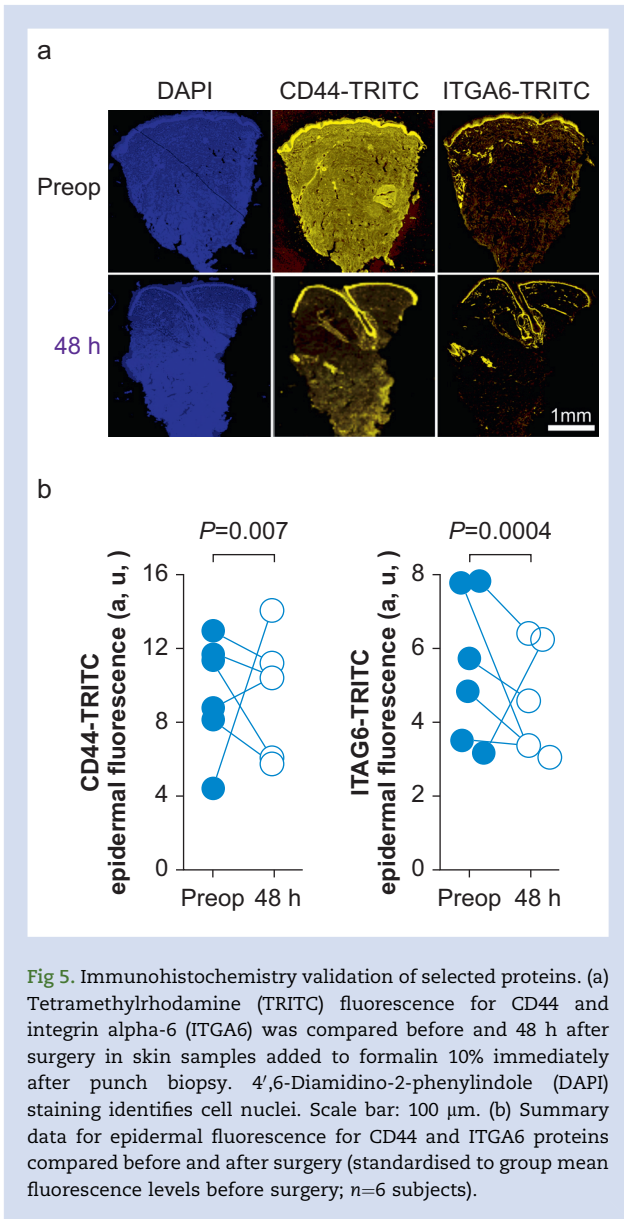


**Fig 5.** Immunohistochemistry validation of selected proteins. (a) Tetramethylrhodamine (TRITC) fluorescence for CD44 and integrin alpha-6 (ITGA6) was compared before and 48 h after surgery in skin samples added to formalin 10% immediately after punch biopsy. 4',6-Diamidino-2-phenylindole (DAPI) staining identifies cell nuclei. Scale bar: 100  $\mu$ m. (b) Summary data for epidermal fluorescence for CD44 and ITGA6 proteins compared before and after surgery (standardised to group mean fluorescence levels before surgery;  $n=6$  subjects).

were exclusively observed in patients where  $DO_2$  was lower, suggesting strongly that failure to supply skin with adequate oxygen during the early perioperative period results in delayed or persistent cellular metabolic stress for at least 36 h after surgery. Our proteomic and immunohistochemical analysis also found decreased postoperative expression of CD44, the epidermal expression of which is required for optimal wound healing by maintaining epidermal elasticity and resistance to stretch, and keratinocyte proliferation and differentiation.<sup>33</sup>

Very few studies have focused on the molecular mechanisms underpinning the association between adequate perioperative  $DO_2$  and reduced morbidity, mortality, or both. Stroke volume-guided fluid and low-dose inotropic therapy were associated with improved  $DO_2$ , microvascular flow, and tissue oxygenation but had no impact on global (plasma) measures of inflammation after major surgery.<sup>34</sup> By contrast, proteomic analysis of skin biopsies obtained after surgery from subjects with normal  $DO_2$  after surgery showed a

coordinated leucocyte activation response that was absent in subjects with low  $DO_2$ . Moreover, normal  $DO_2$  was associated with increased expression of PGLYRP-1, which is expressed primarily in the granules of polymorphonuclear leucocytes and is present in neutrophil extracellular traps.<sup>26</sup> PGLYRP-1 is directly bactericidal for both Gram-positive and Gram-negative bacteria by interacting with cell wall peptidoglycan, rather than permeabilising bacterial membranes.<sup>27</sup>

The ubiquitin–proteasome system degrades intracellular proteins into peptide fragments that can be presented by major histocompatibility complex (MHC) class I molecules. Increased expression of PSMB9 was unique to the low  $DO_2$  group; PSMB9 is one of two critical immunoproteasome subunits that degrade cell proteins to generate peptides for antigen presentation exclusively during acute inflammation.<sup>35</sup> Immunoproteasome expression is closely associated with T-cell infiltration, through cytokine production and T-cell expansion, survival, or both, by regulating apoptotic machinery, transcription factor, or both activation.<sup>36</sup>

We also noted that increased expression of thrombospondin-1 (TSP-1) and plasminogen in both groups. The presence of TSP-1, a potent chemotactic factor for monocytes and neutrophils, in skin biopsy samples 48 h after surgery is consistent with its role in the early inflammatory phase of wounds; absence of TSP-1 delays wound healing.<sup>37</sup> However, given that we did not acquire further biopsy samples beyond 48 h of surgery, we cannot exclude that the deleterious effects of persistently elevated expression of wound bed TSP1 prevents effective wound healing over the longer term.<sup>38</sup> The early presence of plasminogen in postoperative biopsy samples from both groups is also consistent with the critical role of this potent serine protease in triggering the resolution of inflammation and activating the proliferation phase of wound repair.<sup>39</sup> The observed increase in expression of kininogen, through which kinins are formed in the skin by the enzymatic action of tissue kallikrein, is consistent with its role in skin homeostasis, wound healing, and organ dysfunction more widely.<sup>40</sup>

A strength of our study design was the within-subject comparison of punch biopsies within a similar abdominal area, thereby serving as a robust internal control. The masked analysis of samples to trial allocation is another strength. There are several limitations of this ‘first-in-man’ study of surgical patients. Samples obtained as part of a randomised controlled study in a specific subset of patients at higher risk of perioperative morbidity may not be generalisable across all surgical populations. By extension from murine experimental work, we surmised that low global  $DO_2$  would result in lower skin  $DO_2$ , but this was not directly measured in skin. The proteins selected for immunohistochemical validation represent only a small subset of the proteins impacted by surgery; they were chosen based on the availability of validated antibodies for immunohistochemistry, systems biology analysis, and literature supporting a link with skin-specific pathology. Because of cost and patient-related constraints, further samples beyond 48 h after surgery were not obtained during the proliferative reparative phase. Usually, punch biopsies heal 5–10 days after the procedure, which would have lent itself to monitoring the rate of healing if the subjects had been guaranteed to reside in hospital until the punch biopsy site had healed. A derivation-validation approach correlated with postoperative outcomes would add further value.

In summary, serial skin biopsies identified novel surgery-specific protein changes in adults undergoing major elective



noncardiac surgery. This approach may identify potential biomarkers with clinical utility, particularly as we observed upregulation of biomarkers over time. Proteomic analysis of skin biopsies provides further understanding of perioperative end-organ dysfunction, including the potential development of precision medicine-guided treatments for wound healing after major surgery.<sup>41</sup>

## Authors' contributions

Study design: GLA

Study conduct: SI, LGP, AJT, AGDA, GLA, KM, WEH

Experiments: WEH, EB, FB, TJ, AGDA, KM, GLA

Data analysis: WEH, FB, MC, EAT, AGDA, GLA, KM

Drafting/revising manuscript: GLA, WEH, MC, TJ, AJT, AGDA, EAT, KM

## Funding

UK National Institute for Health Research (NIHR) Great Ormond Street Hospital Biomedical Research Centre. Academy of Medical Sciences/Health Foundation Clinician Scientist Award CSF3 (GLA); British Oxygen Company research chair grant in Anaesthesia (GLA); Great Ormond Street Hospital Biomedical Research Centre (EB, WH, KM); British Heart Foundation: (PG/17/40/33028) (MC); UK National Institute for Health Research (GLA); Barts Charity (TJ).

## Declarations of interest

GLA is an Editor of *British Journal of Anaesthesia*; and declares consultancy work for GlaxoSmithKline, unrelated to this work.

## Appendix A. Supplementary data

Supplementary data to this article can be found online at <https://doi.org/10.1016/j.bja.2021.06.003>.

## References

- Zhang B, Whiteaker JR, Hoofnagle AN, Baird GS, Rodland KD, Paulovich AG. Clinical potential of mass spectrometry-based proteogenomics. *Nat Rev Clin Oncol* 2019; **16**: 256–68
- Bantscheff M, Lemeer S, Savitski MM, Kuster B. Quantitative mass spectrometry in proteomics: critical review update from 2007 to the present. *Anal Bioanal Chem* 2012; **404**: 939–65
- Fong TG, Chan NY, Dillon ST, et al. Identification of plasma proteome signatures associated with surgery using SOMAscan. *Ann Surg* 2021; **273**: 732–42
- Mukai A, Suehiro K, Watanabe R, et al. Impact of intraoperative goal-directed fluid therapy on major morbidity and mortality after transthoracic oesophagectomy: a multicentre, randomised controlled trial. *Br J Anaesth* 2020; **125**: 953–61
- Khuri SF, Henderson WG, DePalma RG, Mosca C, Healey NA, Kumbhani DJ. Determinants of long-term survival after major surgery and the adverse effect of postoperative complications. *Ann Surg* 2005; **242**: 326–41
- Wu WC, Smith TS, Henderson WG, et al. Operative blood loss, blood transfusion, and 30-day mortality in older patients after major noncardiac surgery. *Ann Surg* 2010; **252**: 11–7
- Pearse RM, Harrison DA, MacDonald N, et al. Effect of a perioperative, cardiac output-guided hemodynamic therapy algorithm on outcomes following major gastrointestinal surgery: a randomized clinical trial and systematic review. *JAMA* 2014; **311**: 2181–90
- Ackland GL, Iqbal S, Paredes LG, et al. Individualised oxygen delivery targeted haemodynamic therapy in high-risk surgical patients: a multicentre, randomised, double-blind, controlled, mechanistic trial. *Lancet Respir Med* 2015; **3**: 33–41
- Peerless JR, Alexander JJ, Pinchak AC, Piotrowski JJ, Malangoni MA. Oxygen delivery is an important predictor of outcome in patients with ruptured abdominal aortic aneurysms. *Ann Surg* 1998; **227**: 726–32. ; discussion 32–4
- Hotamisligil GS. Inflammation, metaflammation and immunometabolic disorders. *Nature* 2017; **542**: 177–85
- Jonsson K, Jensen JA, Goodson 3rd WH, et al. Tissue oxygenation, anemia, and perfusion in relation to wound healing in surgical patients. *Ann Surg* 1991; **214**: 605–13
- Catania RA, Schwacha MG, Cioffi WG, Bland KI, Chaudry IH. Does uninjured skin release proinflammatory cytokines following trauma and hemorrhage? *Arch Surg* 1999; **134**: 368–73. ; discussion 73–4
- Bos JD. The skin as an organ of immunity. *Clin Exp Immunol* 1997; **107**(Suppl 1): 3–5
- Kabashima K, Honda T, Ginhoux F, Egawa G. The immunological anatomy of the skin. *Nat Rev Immunol* 2019; **19**: 19–30
- Hope JC, Dearman RJ, Kimber I, Hopkins SJ. The kinetics of cytokine production by draining lymph node cells following primary exposure of mice to chemical allergens. *Immunology* 1994; **83**: 250–5
- Clavien PA, Strasberg SM. Severity grading of surgical complications. *Ann Surg* 2009; **250**: 197–8
- Bliss E, Heywood WE, Benatti M, Sebire NJ, Mills K. An optimised method for the proteomic profiling of full thickness human skin. *Biol Proced Online* 2016; **18**: 15
- Distler U, Kuharev J, Navarro P, Levin Y, Schild H, Tenzer S. Drift time-specific collision energies enable deep-coverage data-independent acquisition proteomics. *Nat Methods* 2014; **11**: 167–70
- Geromanos SJ, Vissers JP, Silva JC, et al. The detection, correlation, and comparison of peptide precursor and product ions from data independent LC-MS with data dependant LC-MS/MS. *Proteomics* 2009; **9**: 1683–95
- Perez-Riverol Y, Csordas A, Bai J, et al. The PRIDE database and related tools and resources in 2019: improving support for quantification data. *Nucleic Acids Res* 2019; **47**: D442–50
- Szklarczyk D, Gable AL, Lyon D, et al. STRING v11: protein-protein association networks with increased coverage, supporting functional discovery in genome-wide experimental datasets. *Nucleic Acids Res* 2019; **47**: D607–13
- The Gene Ontology Consortium. The gene Ontology resource: 20 years and still GOing strong. *Nucleic Acids Res* 2019; **47**: D330–8
- Kanehisa M, Sato Y, Furumichi M, Morishima K, Tanabe M. New approach for understanding genome variations in KEGG. *Nucleic Acids Res* 2019; **47**: D590–5
- Huang da W, Sherman BT, Lempicki RA. Systematic and integrative analysis of large gene lists using DAVID bioinformatics resources. *Nat Protoc* 2009; **4**: 44–57

25. Kramer A, Green J, Pollard Jr J, Tugendreich S. Causal analysis approaches in ingenuity pathway analysis. *Bioinformatics* 2014; **30**: 523–30
26. Cho JH, Fraser IP, Fukase K, et al. Human peptidoglycan recognition protein S is an effector of neutrophil-mediated innate immunity. *Blood* 2005; **106**: 2551–8
27. Dziarski R, Kashyap DR, Gupta D. Mammalian peptidoglycan recognition proteins kill bacteria by activating two-component systems and modulate microbiome and inflammation. *Microb Drug Resist* 2012; **18**: 280–5
28. Carpenter S. Skin biopsy for diagnosis of hereditary neurologic metabolic disease. *Arch Dermatol* 1987; **123**: 1618–21
29. de Veer SJ, Furio L, Harris JM, Hovnanian A. Proteases and proteomics: cutting to the core of human skin pathologies. *Proteomics Clin Appl* 2014; **8**: 389–402
30. Gurtner GC, Werner S, Barrandon Y, Longaker MT. Wound repair and regeneration. *Nature* 2008; **453**: 314–21
31. Werner S, Grose R. Regulation of wound healing by growth factors and cytokines. *Physiol Rev* 2003; **83**: 835–70
32. Spallotta F, Cencioni C, Straino S, et al. A nitric oxide-dependent cross-talk between class I and III histone deacetylases accelerates skin repair. *J Biol Chem* 2013; **288**: 11004–12
33. Shatirishvili M, Burk AS, Franz CM, et al. Epidermal-specific deletion of CD44 reveals a function in keratinocytes in response to mechanical stress. *Cell Death Dis* 2016; **7**: e2461
34. Jhanji S, Vivian-Smith A, Lucena-Amaro S, Watson D, Hinds CJ, Pearse RM. Haemodynamic optimisation improves tissue microvascular flow and oxygenation after major surgery: a randomised controlled trial. *Crit Care* 2010; **14**: R151
35. Kruger E, Kloetzel PM. Immunoproteasomes at the interface of innate and adaptive immune responses: two faces of one enzyme. *Curr Opin Immunol* 2012; **24**: 77–83
36. Thomas C, Tampe R. MHC I chaperone complexes shaping immunity. *Curr Opin Immunol* 2019; **58**: 9–15
37. Agah A, Kyriakides TR, Lawler J, Bornstein P. The lack of thrombospondin-1 (TSP1) dictates the course of wound healing in double-TSP1/TSP2-null mice. *Am J Pathol* 2002; **161**: 831–9
38. Isenberg JS, Pappan LK, Romeo MJ, et al. Blockade of thrombospondin-1-CD47 interactions prevents necrosis of full thickness skin grafts. *Ann Surg* 2008; **247**: 180–90
39. Sulniute R, Shen Y, Guo YZ, et al. Plasminogen is a critical regulator of cutaneous wound healing. *Thromb Haemost* 2016; **115**: 1001–9
40. Chao J, Shen B, Gao L, Xia CF, Bledsoe G, Chao L. Tissue kallikrein in cardiovascular, cerebrovascular and renal diseases and skin wound healing. *Biol Chem* 2010; **391**: 345–55
41. Lisboa FA, Dente CJ, Schobel SA, et al. Utilizing precision medicine to estimate timing for surgical closure of traumatic extremity wounds. *Ann Surg* 2019; **270**: 535–43

Handling editor: Hugh C Hemmings Jr